bioRxiv preprint doi: https://doi.org/10.1101/108878; this version posted February 15, 2017. The copyright holder for this preprint (which was not certified by peer review) is the author/funder. All rights reserved. No reuse allowed without permission.

Running Head: Mutual gaze increases infant-adult connectivity

Speaker gaze changes information coupling between infant and adult brains

Victoria Leong[1,2], Elizabeth Byrne[3], Kaili Clackson[1], Sarah Lam[1] & Sam Wass[4]

.

[1]*Department of Psychology, University of Cambridge*

[2] *Nanyang Technological University, Singapore*

[3] *MRC Cognition & Brain Sciences Unit, Cambridge*

[4] *University of East London*

Corresponding Author:

Victoria Leong

Department of Psychology, Downing Street

Cambridge CB2 3EB, U.K.

Tel. 44 1223 333550 Fax. 44 1223 333564

Email: vvec2@cam.ac.uk

bioRxiv preprint doi: https://doi.org/10.1101/108878; this version posted February 15, 2017. The copyright holder for this preprint (which was not certified by peer review) is the author/funder. All rights reserved. No reuse allowed without permission.

ABSTRACT

In infants, as in adults, social context is known to influence attentional allocation during communication. The sharing of attention between individuals potentiates learning, but little is understood about the interpersonal neural mechanisms that support this process. Recently, it has been demonstrated that during spoken communication, spontaneous neural coupling (temporal synchronization) arises between speaker and listener, and their coupling strength predicts communicative success. Here, we assess whether gaze, a salient cue that elicits joint attention, moderates endogenous levels of neural coupling in adult-infant speaker-listener dyads. Electroencephalography (EEG) was concurrently measured in 19 adult experimenter-infant dyads at left and right central electrode locations. The adult sang nursery rhymes to the infant whilst either looking directly at the infant, or with her gaze averted by 20°. Gaze-related changes in adult-infant neural network connectivity were measured using Partial Directed Coherence (PDC), a statistical measure of causality and directional influence. Our results showed that bi-directional connectivity between adults and infants was significantly higher during periods of Direct than Indirect gaze in Theta, Alpha and Beta EEG bands. Further analyses suggested that these effects were not attributable to differences in task engagement, EEG power, or basic neural processing of speech between gaze conditions. Further, in Alpha and Beta bands, but not other bands, infants influenced adults more strongly than *vice versa*. This is the first demonstration that mutual direct gaze increases adult-infant neural coupling during social communication. Future research should explore the role of neural coupling in learning and other aspects of social behavior.

(248/250 words)

Keywords: Neural synchronization, dyadic interaction, mutual gaze, joint attention

bioRxiv preprint doi: https://doi.org/10.1101/108878; this version posted February 15, 2017. The copyright holder for this preprint (which was not certified by peer review) is the author/funder. All rights reserved. No reuse allowed without permission.

SIGNIFICANCE STATEMENT

During infancy, the social context exerts powerful influences on learning. This context arises from dynamic interactions between social partners, yet all known neural infancy studies have only considered what occurs within one partner, the infant. Consequently, the *contingency* (temporal dependency) of infant's neural activity on the adult's and vice versa has never been measured. Yet, recent adult studies suggest that strong interpersonal neural contingency (coupling) predicts successful communication. Here, we report the first ever study to examine adult-infant neural coupling and characterize its causal architecture. We observed strong bi-directional adult-infant coupling which was significantly modulated by social gaze. These results are important because they challenge the current thinking about how social effects on early learning are understood and investigated.

(119/120 words)

bioRxiv preprint doi: https://doi.org/10.1101/108878; this version posted February 15, 2017. The copyright holder for this preprint (which was not certified by peer review) is the author/funder. All rights reserved. No reuse allowed without permission.

1 INTRODUCTION

Social interactions between adults and infants involve both verbal and non-verbal modes of communication (Csibra & Gergely, 2009). These are known to play a vital role in supporting early learning across multiple domains of language, cognition and socio-emotional development (Rogoff, 1990; Leslie, 1994; Csibra & Gergely, 1998). The neural mechanisms that support these social interactions are now beginning to be understood. Speech perception, for example, is known to involve the synchronization (or phase-locking) of neural activity to temporal structures in speech (Giraud & Poeppel, 2012). Infants, like adults, show neural oscillatory phase-locking to speech (Leong et al., in revision; see also Telkemeyer et al, 2009).

Infants are also known to rely heavily on non-verbal cues (such as eye contact, gaze direction, pointing and gestures) to infer meaning, intention and causality (Csibra & Gergely, 2000). Neonates are already sensitive to adults' non-verbal social communicative cues (Meltzoff & Moore, 1977; Farroni et al, 2002) but the ability to engage in non-verbal communication develops rapidly over the first year of life (Mundy et al, 2000, 2003). A highly salient ostensive signal in human communication is direct gaze towards the addressee, which usually results in mutual eye contact (Csibra & Gergely, 2009). From birth, infants prefer to look at pictures of faces with direct gaze over averted gaze (Farroni et al., 2002). By 4 months, ERP studies show enhanced neural processing of pictures of faces showing direct relative to indirect gaze (Farroni et al., 2002). In adults, direct gaze leads to activation in similar neural areas as those evoked by other communicative signals (e.g. direct gaze vs eye-brow raise), which are both interpreted as ostensive signals (Kampe et al., 2003).

bioRxiv preprint doi: https://doi.org/10.1101/108878; this version posted February 15, 2017. The copyright holder for this preprint (which was not certified by peer review) is the author/funder. All rights reserved. No reuse allowed without permission.

Direct gaze potentiates joint attention (a state of shared focus between individuals), which in turn enhances infants' neural processing of jointly-attended stimuli. For example, infants are more likely to follow an adult's gaze towards another object when it is preceded by a moment of direct, mutual gaze (Senju & Csibra, 2008). When infants attend jointly to an object with an adult, they show a larger Nc ERP (Striano et al., 2006; Parise et al., 2010), along with changes in neural activity in Theta- and Alpha- EEG bands (Hoehl et al., 2014; St John et al., 2016). However, joint attention is a dyadic activity, and previous investigations into the neural correlates of joint attention have, almost exclusively, only explored the neural correlates of joint attention within the child alone (although see Lachat et al, 2012). Consequently, the *contingency* (temporal dependency) of one partner's neural activity with respect to the other during joint attention has not previously been investigated.

Adult-infant temporal contingencies have long been observed in behavioural and physiological domains. For example, patterns of temporally synchronous activity between parent and child during shared attention have been noted both for gaze (Kaye & Fogel, 1980) and affect (Cohn & Tronick, 1988; Feldman et al., 2006). These episodes of interaction also lead to physiological synchronization of heart rhythms (Feldman et al., 2011). Interpersonal *neural* dynamics, however, are only just beginning to be studied using neuroimaging methods that allow the simultaneous capture of brain activity between two individuals, such as dual electroencephalography (dual-EEG; e.g. Dumas et al, 2010, 2012; Lachat et al, 2012), dual functional magnetic resonance imaging (dual-fMRI; e.g. Stephens et al, 2010; Anders et al, 2011) and dual functional near infrared spectroscopy (dual-fNIRS; e.g. Jiang et al., 2012), see Hasson et al (2012), Hari et al (2013) and Koike et al (2015) for recent reviews.

In adults, neural synchronisation between individuals has been shown in frontal areas during face-to-face communication (Jiang et al, 2012). Further, the *strength* of speaker-listener

bioRxiv preprint doi: https://doi.org/10.1101/108878; this version posted February 15, 2017. The copyright holder for this preprint (which was not certified by peer review) is the author/funder. All rights reserved. No reuse allowed without permission.

neural synchronisation has been associated with listeners' success in comprehending the speaker (Stephens et al, 2010; Dikker et al, 2014; Silbert et al, 2014). Neural synchronization between adults has also been observed in the absence of speech. For example, Saito et al (2010) found that adult pairs who performed a gaze cueing task in real time together, maintaining eye contact and gaze following, had stronger mutual neural synchronization in their right inferior frontal gyri (IFG) than control data from non-matched pairs.

Here, we aimed to measure the temporal dependency (synchronization) between adult and infant neural signals during conditions of direct or indirect adult speaker gaze. The measure we used was Partial directed coherence (PDC), which not only captures the *strength* of instantaneous interactions between pairs of neural signals, but also provides insights into their *causal* relationship and *direction* of influence (Baccala & Sameshima, 2001; Baccala et al, 2007; Faes & Nollo, 2010, 2011). PDC is based on the concept of Granger causality (Granger, 1969) which reflects the extent to which one signal *statistically predicts* another signal in time. Further, PDC reveals only *direct* couplings between channels (e.g. i -> j), and does not measure the effect of intermediary channels (e.g. i -> k -> j). Thus, PDC is a suitable measure of changes in information flow (both directionality and strength) during different network states. Here, we apply the PDC metric to measure the causal architecture and information flows in a dyadic social network comprising an infant and an adult. We manipulate social context so that the adult is either looking directly at the infant, or indirectly, at a 20° oblique angle.

In terms of affect and physiological changes, research has shown that the influence of infants and parents on one another is bi-directional (Feldman et al., 2006, 2011). In older infants, however, such as the age range studied here, research suggests that mothers are more likely to be responsive to their children than *vice versa* (Cohn & Tronick, 1986.)
Accordingly, we predicted that: i) significant neural coupling would exist between adults and

bioRxiv preprint doi: https://doi.org/10.1101/108878; this version posted February 15, 2017. The copyright holder for this preprint (which was not certified by peer review) is the author/funder. All rights reserved. No reuse allowed without permission.

infants during social interaction, ii) that direct gaze would be associated with higher interpersonal neural connectivity than indirect gaze and iii) that infants would influence adults more than *vice versa*.

2 METHODS

2.1 Participants

The participants were twenty-nine infants (15M/14F) and one female adult experimenter. The infants' mothers were all native English speakers. The median age was 8.3 months (st. err. 0.44 months). All infants had no neurological problems and had normal hearing and vision, as assessed by maternal report.

2.2 Materials

Seven familiar nursery rhymes such as 'Old MacDonald' were used as sung stimuli, as listed in Table S1 (Supplementary materials). Prior to starting the experiment, mothers confirmed that the nursery rhymes were familiar to their infant. As the stimuli were produced live the experimenter was recorded during each experimental session to ensure that the durations were consistent between the Direct and Indirect conditions (see Table S1). Bonferroni-corrected t-tests did not identify any significant differences between conditions.

2.3 Protocol

Infants sat upright in a high chair facing the female experimenter, who was the same for all testing sessions. Each nursery rhyme was presented in two gaze conditions. In the Direct condition the experimenter looked directly at the infant while singing; in the Indirect condition she averted her gaze by fixating at a constant visual target exactly 20° to the left or right side of the infant (see Figure 1). The experiment was divided into two blocks, with a

bioRxiv preprint doi: https://doi.org/10.1101/108878; this version posted February 15, 2017. The copyright holder for this preprint (which was not certified by peer review) is the author/funder. All rights reserved. No reuse allowed without permission.

short break in-between. In each block, the experimenter sang each nursery rhyme to the infant twice (once Direct and once Indirect, order counterbalanced). Thus, infants heard each nursery rhyme 4 times in total. The total stimulus presentation time (7 nursery rhymes x 4 repetitions) was 377.65 seconds on average (range = 350.73s to 391.90s, SD = 12.42s).

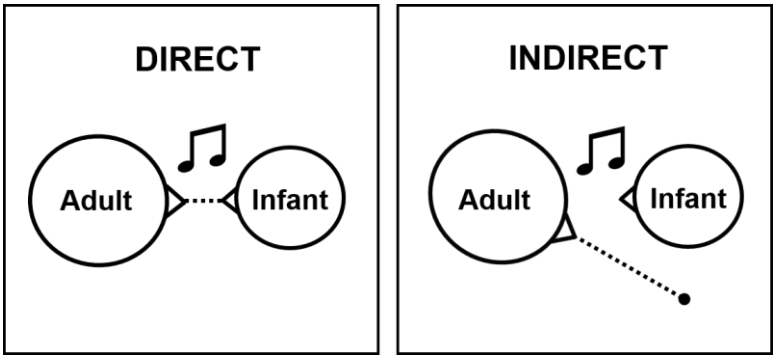

Figure 1. Illustration of a top-down view of the adult and infant during Direct and Indirect gaze conditions. Dotted lines indicate the direction of the adult's gaze.

2.4 EEG acquisition

EEG was recorded simultaneously from the infant and the female adult experimenter from two electrodes in the central region (C3 and C4), referenced to the vertex (Cz) according to the International 10–20 placement system. EEG was recorded from central sites to reduce potential confounding influences of muscle artefacts and blinking while still capturing a robust neural response. The vertex reference location was used because it produces comparable results to other reference sites (Tomarken, Davidson, Wheeler, & Kinney, 1992), and is the least invasive for young infants. Prior to electrode attachment, electrode sites were marked and wiped with alcohol. Electrodes were then affixed to the scalp using Signa conductive electrode gel (Parker Laboratories Inc, NJ). EEG signals were obtained using a Biopac MP150 Acquisition System with filters at 0.1 Hz highpass and 100 Hz lowpass. Wireless dual-channel BioNomadix amplifiers were used to reduce distraction

bioRxiv preprint doi: https://doi.org/10.1101/108878; this version posted February 15, 2017. The copyright holder for this preprint (which was not certified by peer review) is the author/funder. All rights reserved. No reuse allowed without permission.

for the infant during testing. EEG was recorded at 1000 Hz using AcqKnowledge software (Biopac Systems Inc). All further analysis was performed using Matlab software (Mathworks Inc). Both participants' data was recorded concurrently in a single acquisition session on the same computer, ensuring accurate time synchronization of the two data streams.

2.5 EEG artifact rejection and pre-processing

To ensure that the EEG data used for analysis reflected only awake, attentive and movement-free behaviour we performed a two-stage artifact rejection procedure. First, each dyad was video-taped and the videos were reviewed frame-by-frame (30 fps) to identify the onset and offset times of movement artifacts, including blinks, head and limb motion, and chewing. Only periods when infants were still and looking directly at the experimenter were accepted. Next, manual artifact rejection was performed on this still, attentive data to further exclude segments where the amplitude of infants' or adults' EEG exceeded +100 μV.

Following this two-stage process, 19/29 infants (10M/9F), gave sufficient data for inclusion in the final analyses. The median (st.err.) age of retained infants was 8.52 (0.57) months. On average, the retained infants contributed 45.52 seconds (range = 8.00s to 107.00s, SD = 28.18s) of still and attentive data in the Direct gaze condition, and 43.92 seconds (range = 11.00 to 122.62s, SD = 30.07s) in the Indirect gaze condition. Adult data was only analysed for those segments in which the infant data were retained. A paired t-test confirmed that there was no significant difference in the amount of still and attentive data collected between Direct and Indirect gaze conditions ($t(18) = 0.44$, $p = .66$). Therefore, infants were not more inattentive during the Indirect gaze condition.

The cleaned EEG data was resampled to a lower frequency of 200 Hz, which permitted the use of a low order multivariate autoregressive (MVAR) model in the

bioRxiv preprint doi: https://doi.org/10.1101/108878; this version posted February 15, 2017. The copyright holder for this preprint (which was not certified by peer review) is the author/funder. All rights reserved. No reuse allowed without permission.

subsequent connectivity analysis, whilst retaining sufficient spectral detail. The data was then low-pass filtered under 45 Hz to suppress electrical line noise. Finally, the data was segmented into 1.0s-long epochs (200 data samples per epoch) for connectivity analysis.

2.6 EEG analyses : Power spectrum and GPDC network connectivity

A detailed description of all methods is given in the Supplementary Materials (Section 2). Briefly, we first assessed the EEG power spectrum of infant and adult signals for each experimental condition and hemisphere (left or right). Second, to assess network connectivity in each gaze condition, we measured Generalised Partial Directed Coherence (GPDC), which is a directional casual measure of direct information flows between channels in a network (Baccala & Sameshima, 2001; Baccala et al, 2007; Faes & Nollo, 2010, 2011). The GPDC measure is based on the principles of Granger Causality (Granger, 1969), and measures the degree of influence that channel j ('Sender') *directly* has on channel i ('Receiver') with respect to the total influence of j on all channels in the network. Here, each individual electrode (Infant L, Infant R, Adult L, Adult R) was taken as one channel (see Figure 2). We computed directed coherence values for all 12 possible (non-self) pairwise connections, both within individual (e.g. Infant L -> Infant R) as well as across individuals (e.g. Infant L -> Adult L).

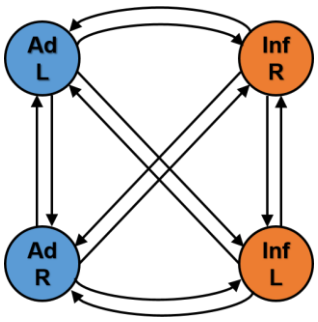

Figure 2. Network depiction of the 4 electrode channels (nodes) and their 12 possible pairwise connections (edges).

bioRxiv preprint doi: https://doi.org/10.1101/108878; this version posted February 15, 2017. The copyright holder for this preprint (which was not certified by peer review) is the author/funder. All rights reserved. No reuse allowed without permission.

2.7 Control analyses

In the first control analysis, we generated a surrogate dataset comprising all 3876 possible combinations of *non-matched* adult-infant data (i.e. combinations of adult and infant data from different experimental sessions). We then performed an identical connectivity analysis on this surrogate dataset (see Supplementary Materials Section 2.2). The resulting values provided a baseline measure of the 'random' level of coherence that did not specifically arise from the task (e.g. due to being present in a similar physical testing environment). In the second control analysis, we examined whether basic sensory processing of the speech stimulus differed between Direct and Indirect mutual gaze conditions. If basic auditory processing differences were present, then any observed neural connectivity changes would not be solely gaze-related. Accordingly, wavelet coherence between the neural EEG signal and the speech amplitude envelope was measured in each gaze condition for adults and infants. A description of this method is given in the Supplementary Materials (Section 2.3).

2.8 Statistical analysis of GPDC network changes

To assess whether the Gaze experimental manipulation resulted in statistically-significant changes in GPDC strength within the neural network, we conducted 2 x 2 x 2 x 2 x 2 Mixed ANOVAs taking Gaze condition ([2], Direct or Indirect), 'Sender' ([2], Infant or Adult), 'Sending' Hemisphere ([2], L or R) and 'Receiving' Hemisphere ([2], L or R) as within-subjects factors. This allowed us to determine whether there was an overall global effect of Gaze (as indexed by a significant main effect of Gaze), and also whether patterns of connections in the network displayed a consistent causal architecture. For example, if adults were influencing infants more strongly than infants were influencing adults overall, this would be indexed by a significant main effect of 'Sender'. Table S2 (Supplementary Materials) summarises the predicted pattern of effects. In addition, we also examined whether

bioRxiv preprint doi: https://doi.org/10.1101/108878; this version posted February 15, 2017. The copyright holder for this preprint (which was not certified by peer review) is the author/funder. All rights reserved. No reuse allowed without permission.

there were differences in connectivity as a function of infant age by using a median split at 9 months, and entering Age Group as a between-subjects factor in the ANOVA analysis. Finally, infants' mean looking time across all conditions was entered as a co-variate, to control for individual differences in infant attentiveness.

3 RESULTS

3.1 Analysis of EEG power spectra across conditions

Figure 3 shows the mean power spectrum of the EEG signal for infants and adults, for the experimental conditions of Direct (solid line) and Indirect (dotted line) gaze, for left and right hemispheres respectively. Paired t-tests conducted for each EEG frequency band (Delta [1-3 Hz], Theta [3-6 Hz], Alpha [6-9 Hz], Beta [9-25 Hz], and Gamma [25-40 Hz]) indicated that there was no significant difference in EEG power between the Direct and Indirect conditions in infant or adult signals for either hemisphere in any EEG band (p>.05 for all comparisons, Benjamini-Hochberg FDR-corrected [Benjamini & Hochberg, 1995, 2000]). Therefore, the gaze manipulation did not generate any detectable power changes that might systematically bias the PDC metric (see Supplementary Materials 2.1 for an explanation of the effect of power on PDC).

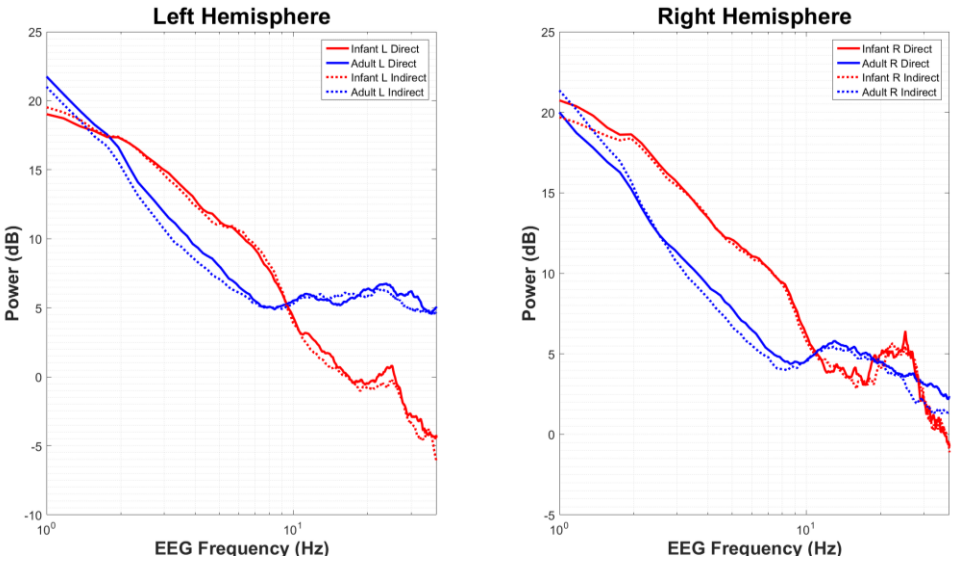

bioRxiv preprint doi: https://doi.org/10.1101/108878; this version posted February 15, 2017. The copyright holder for this preprint (which was not certified by peer review) is the author/funder. All rights reserved. No reuse allowed without permission.

Figure 3. Raw EEG spectra for infant (red) and adult (blue) signals, for Direct (solid line) and Indirect (dotted line) gaze conditions. EEG frequency is shown on the x-axis and power is shown on the y-axis. Left and right hemisphere channels are plotted in left and right subplots respectively.

3.2 Comparison of real and non-matched control surrogate data

The mean GPDC values for each EEG band, for each pairwise connection, are shown in Figure 4 (full values are given in Tables S3 and S4 of the Supplementary Materials). We assessed whether the mean GPDC values for each non-self pairwise connection, and for each condition and each EEG frequency, were significantly above their respective threshold values established from the surrogate dataset with non-matched adult-infant pairs. One-sample t-tests revealed that all real GPDC values were significantly above their respective surrogate values for all frequencies and non-self pairwise connections (Benjamini-Hochberg FDR-corrected p<.05 for all pairwise connections [Benjamini & Hochberg, 1995, 2000]). Therefore, significant bi-directional patterns of connectivity occurred both *across* and *within* infant and adult signals in all EEG bands.

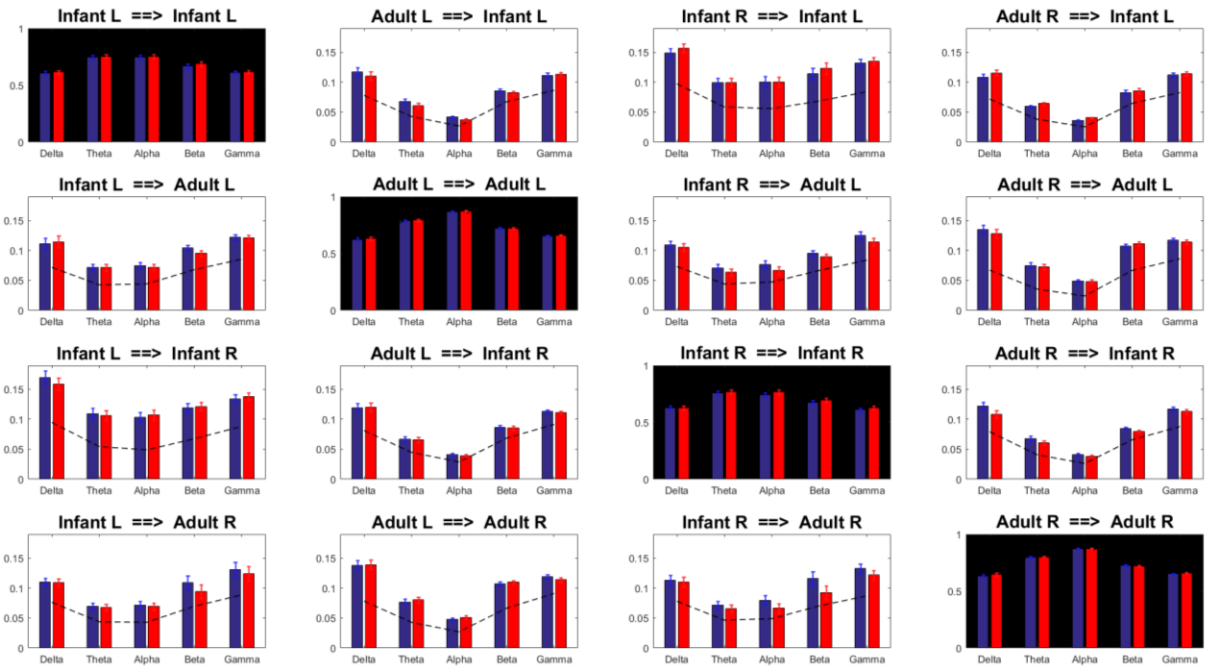

bioRxiv preprint doi: https://doi.org/10.1101/108878; this version posted February 15, 2017. The copyright holder for this preprint (which was not certified by peer review) is the author/funder. All rights reserved. No reuse allowed without permission.

Figure 4. Group mean GPDC values for each EEG band for each pairwise connection, for Direct gaze (blue) and Indirect gaze (red) conditions. Columns indicate 'Senders' and rows indicate 'Receivers' (e.g. the leftmost column shows all connections where the Infant L channel is the 'Sender', and each row is a different 'Receiver'. For this leftmost column, the 2nd and 4th row are connections across individuals [e.g. Inf L -Ad L] whereas the 3rd row is a within-individual connection [i.e. Inf L – Inf R]). Corresponding threshold values obtained from the surrogate data are plotted as dotted lines. Error bars show the standard error of the mean.

For illustration, Figure 5 depicts a network representation of Alpha band (6-9 Hz) data, where nodes are channels (electrodes) and edges are pairwise GPDC connections. Network graphs for Direct and Indirect gaze conditions are shown in separate subplots, along with the *difference* between conditions (a positive value indicates higher connectivity in the Direct condition). Inspection of Figure 5 indicates that stronger Alpha connectivity was observed in the Direct gaze condition as compared to the Indirect gaze condition in the majority of across-individual connections. Further, infant→adult GPDC values (shown in red) were generally higher than adult→infant values (shown in blue) for the same pairwise connection (e.g. in the Direct condition, Ad L→Inf L = 0.42 whereas Inf L→Ad L = 0.75).

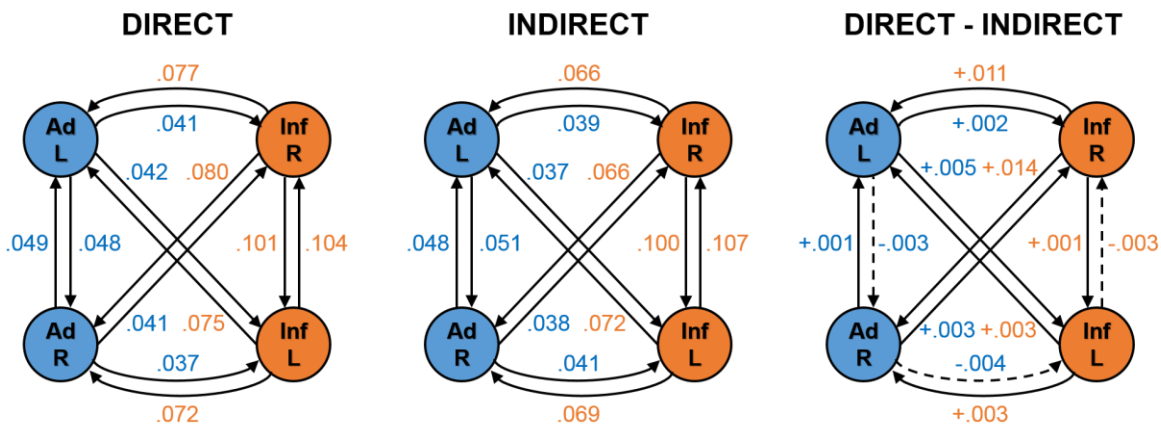

bioRxiv preprint doi: https://doi.org/10.1101/108878; this version posted February 15, 2017. The copyright holder for this preprint (which was not certified by peer review) is the author/funder. All rights reserved. No reuse allowed without permission.

Figure 5. Network depiction of adult-infant connectivity in the Alpha band (6-9 Hz), plotting original GPDC values for Direct (left subplot) and Indirect (middle subplot) conditions, and differenced GPDC values (right subplot). Nodes are electrodes, edges are pairwise connections. Numerical values indicate the GPDC (or differenced) value, where adult 'sending' values are shown in blue and infant 'sending' values are shown in red. For the difference network (right subplot), a solid line indicates a positive difference (Direct > Indirect) and a dashed line indicates a negative difference (Direct < Indirect).

3.3 Network connectivity patterns and modulation by gaze

As outlined previously, Mixed Design ANOVAs were used to assess specific features of network connectivity (such as 'Sender'-'Receiver' patterns and hemispheric lateralization patterns), and the modulation of these connectivity patterns by Gaze. To assess *across*-individual (interpersonal) neural connectivity patterns, five separate ANOVA analyses were conducted for Delta, Theta, Alpha, Beta and Gamma frequency bands. To assess *within*-individual connectivity patterns, a separate set of five ANOVAs were again conducted for Delta, Theta, Alpha, Beta and Gamma bands. The full results of these ANOVAs are reported in the Supplementary Materials (Table S5), and a summary of the major effects is presented here.

3.3.1 Gaze effects

Stronger low-frequency interpersonal connectivity for Direct gaze than Indirect gaze. Overall interpersonal connectivity was significantly stronger for Direct as compared to Indirect gaze in Theta, Alpha and Beta bands (Theta : $F(1,16) = 5.40$, $p<.05$, $\eta^2p = .25$; Alpha : $F(1,16) = 7.94$, $p<.05$, $\eta^2p = .33$; Beta : $F(1,16) = 7.95$, $p<.05$, $\eta^2p = .33$) (see Figure 6). No significant interactions were observed between Gaze and Hemisphere or Age Group in any

bioRxiv preprint doi: https://doi.org/10.1101/108878; this version posted February 15, 2017. The copyright holder for this preprint (which was not certified by peer review) is the author/funder. All rights reserved. No reuse allowed without permission.

EEG band (see Table S5). This suggests that the overall increase in interpersonal neural connectivity for Direct relative to Indirect gaze was consistently observed across left and right hemispheres, and in both younger and older infants. In the Alpha and Beta bands, a marginally non-significant interaction between Gaze and 'Sender' was observed (Alpha : $F(1,16) = 4.01$, $p=.06$, $\eta^2p =.20$; Beta ($F(1,16) = 4.30$, $p=.05$, $\eta^2p = .21$). Tukey post hoc analyses of this interaction indicated that in both bands, infants were stronger 'Senders' in the Direct as compared to the Indirect gaze condition ($p<.05$ for both bands), but the difference between conditions for the adult was not significant. In the Theta band, however, the Gaze x Sender interaction was not significant ($F(1,16) = .13$, $p=.73$, $\eta^2p =.01$) indicating that *both* adult and infant were sending more strongly in the Direct condition.

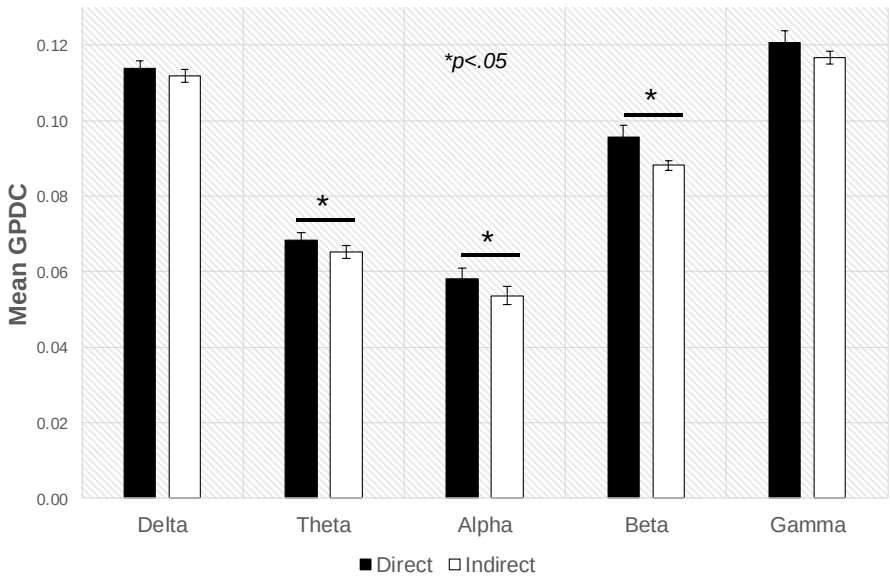

Figure 6. Overall across-individual GPDC strength in Direct and Indirect gaze conditions, for all EEG bands. Error bars show the standard error of the mean.

3.3.2 Direction of adult-infant influences

Infants influence adults more strongly at Alpha and Beta frequencies. In Alpha and Beta bands, infants were stronger 'Senders' than adults (Alpha : $F(1,16) = 7.35$, $p<.05$, $\eta^2p =$

bioRxiv preprint doi: https://doi.org/10.1101/108878; this version posted February 15, 2017. The copyright holder for this preprint (which was not certified by peer review) is the author/funder. All rights reserved. No reuse allowed without permission.

.32; Beta : $F(1,16) = 7.41$, $p<.05$, $\eta^2p = .32$). By contrast, in the Delta, Theta and Gamma bands, there was no significant main effect of 'Sender', indicating that infants and adults were influencing each other equally at these frequencies (Delta : $F(1,16) = 0.02$, $p=.90$, $\eta^2p =.00$; Theta : $F(1,16) = 0.56$, $p=.46$, $\eta^2p =.03$; Gamma : $F(1,16) = 2.87$, $p=.11$, $\eta^2p = .15$).

In the Supplementary Materials Section 5.3 we also describe the results of the *within*-individual connectivity analyses. In brief, stronger within-individual connectivity was observed in infants than adults in four out of five frequency bands assessed (all except Beta). Further, for both infants and adults, stronger within-individual connectivity was observed for Direct gaze relative to the Indirect gaze in the Delta band, but not in other EEG bands. Finally, in the Supplementary Materials Section 6 we describe the results of the second control analysis. This was conducted to examine whether interpersonal connectivity gaze effects could be attributed to differences in basic speech processing (see Figure S1). In brief, no significant differences in speech-brain coherence were observed between the Direct and Indirect gaze conditions at any EEG frequency.

4 DISCUSSION

Recently, neural coupling (synchronization) between adults has been observed during social interaction. For example, previous studies using dual-fMRI have shown that when two adults engage in eye contact, neural activity in areas such as the right inferior frontal gyrus becomes synchronized (Saito et al, 2010; Tanabe et al, 2012). Here, we aimed to (1) determine whether neural coupling also exists between adults and infants during social interaction, (2) to characterize the causal architecture of this coupling, and (3) to assess whether neural coupling is modulated by the social gaze context (direct/indirect gaze).

bioRxiv preprint doi: https://doi.org/10.1101/108878; this version posted February 15, 2017. The copyright holder for this preprint (which was not certified by peer review) is the author/funder. All rights reserved. No reuse allowed without permission.

Our results indicated, first, that significant neural coupling does indeed exist between infants and adults during social interaction. Tests showed that all pairwise coherence values were significantly above their respective surrogate values at all frequencies. That is, one partner's neural activity was temporally dependent on the other partner's neural activity across all timescales measured. Further, when investigating the causal architecture of the adult-infant neural network, we found that each channel (adult or infant; left or right hemisphere) had a significant and direct influence on every other channel, suggesting that causal patterns of influence were bi-directional between adult and infant, and also bi-hemispheric. Of note, significant bi-directional coupling was also observed in the Indirect condition. This was expected, since the infant was facing the adult directly in both conditions, and, for the adult, the infant was positioned at 20° eccentricity from the fixation point, and so still clearly visible.

Second, we found that in Theta, Alpha and Beta bands, stronger adult-infant connectivity was observed during Direct relative to Indirect gaze. This effect was not due to a reduction in attention from the infant listener during adult gaze aversion, as infants showed equivalent time durations of still and attentive looking at the adult across both conditions. This result also cannot be due to underlying power differences in the EEG spectra, as analyses indicated no change in power for infants or adults between the two gaze conditions. The lack of a power effect may initially appear surprising as previous infant studies have reported relative alpha desynchronization in conditions of joint attention (Hoehl et al, 2014; St John et al, 2016). However, it may be the case that alpha desynchronization is only observed in situations involving *triadic* attention between the infant, an adult and an object. Indeed, St John et al (2016) found that when the adult interacted face-to-face with the infant *without* looking or pointing to an object (similar to our current paradigm), no alpha

bioRxiv preprint doi: https://doi.org/10.1101/108878; this version posted February 15, 2017. The copyright holder for this preprint (which was not certified by peer review) is the author/funder. All rights reserved. No reuse allowed without permission.

desynchronization was observed. Our gaze effect also cannot be explained as a meta-phenomenon of changes in basic sensory processing of the speech signal, as both infants' and adults' accuracy of neural tracking of the speech signal remained at the same level across gaze conditions. Third, in Alpha and Beta bands only, we found that infants influenced adults more strongly than *vice versa*. This finding is consistent with behavioural studies which show that mothers are more likely to be responsive to their children than *vice versa* (Cohn & Tronick, 1986). Finally, we found no significant difference in the pattern of effects for younger (<9 months) and older infants, and we also found no overall hemispheric differences in connectivity patterns.

Previous dual-EEG studies on the temporal architecture of interpersonal neural coupling have generally focused on the coordination of motor activities such as finger-tapping tasks (Dumas et al, 2010; Konvalinka et al, 2014; Naeem et al, 2012). Our findings are novel insofar as they were observed in the absence of motor co-ordination within the dyad, but rather as an effect of modulation of social context (gaze). As such our results are most directly comparable to the dual-fNIRS findings from Jiang and colleagues, who observed greater neural synchronization in the left inferior frontal cortex during face-to-face dialog, relative to back-to-back dialog (Jiang et al., 2012). They are also comparable to results from Saito and colleagues who used dual-fMRI and identified, in adults, greater neural synchrony in the inferior frontal gyrus during eye contact. Here, we found that increased adult-infant neural coupling during direct gaze was observed only at low neural oscillatory frequencies such as Theta and Alpha, which are frequency bands that have also been implicated in previous EEG studies of joint attention with infants and adults (Lachat et al, 2012; Hoehl et al, 2014; St John et al, 2016).

bioRxiv preprint doi: https://doi.org/10.1101/108878; this version posted February 15, 2017. The copyright holder for this preprint (which was not certified by peer review) is the author/funder. All rights reserved. No reuse allowed without permission.

One potential mechanism that might mediate interpersonal neural coupling is mutual phase-resetting in response to salient social signals. The *phase* of cortical oscillations (the neural feature with which GPDC values are computed) reflects the excitability of underlying neuronal populations to incoming sensory stimulation (Schroeder et al, 2009). Sensory information arriving during high receptivity periods is more likely to be encoded than information arriving during low receptivity periods. Consequently, neuronal oscillations have been proposed to be a mechanism for temporal and spatial sampling of the environment (Giraud & Poeppel, 2012; Kayser et al, 2012; Lisman, 2005) as well as for attentional selection (Schroeder & Lakatos, 2009). Specifically, salient events in the world are thought to *reset* the phase of on-going neuronal oscillations to match the temporal structure of these events and optimize their encoding (Schroeder & Lakatos, 2009). Consequently, inter-personal neural synchronization could increase within a dyad during the course of social interaction because each partner is continuously producing salient social signals (such as gaze, gestures, or speech) that act as synchronization triggers to reset the phase of their partner's on-going oscillations, bringing each in close alignment with the other. Here, we replicate previous findings with adults that gaze (eye contact) is one social cue that moderates interpersonal neural synchronization.

There are however a number of limitations to this work. The first is that only two EEG channels were recorded from each individual (C3 and C4). While these locations were chosen due to their low contamination by speech articulatory artifacts (see Supplementary Materials Section 7), joint attention is thought to involve a distally distributed neural network of frontal temporal and parietal cortical and subcortical neural regions, which our recording techniques would not capture fully (Mundy, 2003). The advantage of this low-density approach was that it improved the interpretability of the PDC measure, as the number of

bioRxiv preprint doi: https://doi.org/10.1101/108878; this version posted February 15, 2017. The copyright holder for this preprint (which was not certified by peer review) is the author/funder. All rights reserved. No reuse allowed without permission.

pairwise connections increases exponentially with the number of recording channels. Other limitations include possible contamination of our data by the adult's speech articulatory artifacts. As we discuss in detail in the Supplementary Materials (Section 7), these would have been consistent between Direct and Indirect conditions, and therefore a more likely cause of a Type II rather than a Type I statistical error.

In conclusion**,** the current study is (to our knowledge) the first demonstration that significant neural coupling can be measured between infants and adults, and that the strength of adult-infant neural coupling is higher during Direct than Indirect mutual gaze. Further research should aim to assess relationships with attention states, learning and behavior using a wider range of neural recording sites, in more diverse settings, to investigate causal mechanisms, as well as other questions, such as individual differences.

bioRxiv preprint doi: https://doi.org/10.1101/108878; this version posted February 15, 2017. The copyright holder for this preprint (which was not certified by peer review) is the author/funder. All rights reserved. No reuse allowed without permission.

ACKNOWLEDGEMENTS

This research was funded by an ESRC Transforming Social Sciences collaboration grant (ES/N006461/1) to VL and SW, a Lucy Cavendish College Junior Research Fellowship to VL, and by a British Academy Post-Doctoral Fellowship and an ESRC FRL Fellowship (ES/N017560/1) to SW.

bioRxiv preprint doi: https://doi.org/10.1101/108878; this version posted February 15, 2017. The copyright holder for this preprint (which was not certified by peer review) is the author/funder. All rights reserved. No reuse allowed without permission.

BIBLIOGRAPHY

Adhikari, A., Sigurdsson, T., Topiwala, M.A., & Gordon, J.A. (2010). Cross-correlation of instantaneous amplitudes of field potential oscillations: a straightforward method to estimate the directionality and lag between brain areas. J Neurosci Methods, 191:191–200.

Anders, S., Heinzle, J., Weiskopf, N., Ethofer, T., & Haynes, J.D. (2011). Flow of affective information between communicating brains. Neuroimage, 54:439–446.

Anderson, C.W., Stolz, E.A., & Shamsunder, S. (1998). Multivariate autoregressive models for classification of spontaneous electroencephalographic signals during mental tasks. IEEE Trans Biomed Eng, 45 (3), 277-286.

Baccalá, L. & Sameshima, (2001). Partial directed coherence: a new concept in neural structure determination. Biological Cybernetics, 84(6), 463–474.

Baccalá, L., Sameshima, K., Takahashi, D. Y., (2007). Generalized partial directed coherence. In: 15th International Conference on Digital Signal Processing. pp. 163–166.

Benjamini, Y. and Hochberg, Y. (1995). Controlling the false discovery rate: A practical and powerful approach to multiple testing. Journal of the Royal Statistical Society, Series B, 57, 289-300.

Benjamini, Y. and Hochberg, Y. (2000). On the adaptive control of the false discovery rate in multiple testing with independent statistics. Journal of Educational Behavior, Statistics, 25, 60–83.

Brooker, B.H., & Donald, M.W. (1980). Contribution of the speech musculature to apparent human EEG asymmetries prior to vocalization. Brain and Language, 9, 226-245.

bioRxiv preprint doi: https://doi.org/10.1101/108878; this version posted February 15, 2017. The copyright holder for this preprint (which was not certified by peer review) is the author/funder. All rights reserved. No reuse allowed without permission.

Cohn, J. F., & Tronick, E. Z. (1988). Mother-infant face-to-face interaction: Influence is bidirectional and unrelated to periodic cycles in either partner's behavior. Developmental psychology, 24(3), 386.

Corkum, V., & Moore, C. (1998). The origins of joint visual attention in infants. Developmental Psychology, 34(1), 28–38.

Csibra, G. & Gergely, G. (1998). The teleological origins of mentalistic action explanations: A developmental hypothesis. Developmental Science, 1(2), 255-259.

Csibra, G. & Gergely, G. (2009). Natural pedagogy. Trends Cogn. Sci. 13, 148–153.

De Vos, M., Riès, S., Vanderperren, K., Vanrumste, B., Alario, F.X, Van Huffel, S., Burle, B. (2010). Removal of muscle artifacts from EEG recordings of spoken language production. Neuroinformatics, 8, 135-150.

Dikker, S., Silbert, L.J., Hasson, U., Zevin, J.D. (2014). On the same wavelength: predictable language enhances speaker-listener brain-to-brain synchrony in posterior superior temporal gyrus. J Neuroscience 34:6267-6272

Dumas, G.., Nade,l J., Soussignan, R., Martinerie, J., & Garnero, L. (2010). Inter-brain synchronization during social interaction. PLoS ONE 5:e12166 10.1371/journal.pone.0012166

Dumas, G., Martinerie, J., Soussignan, R., & Nadel, J. (2012). Does the brain know who is at the origin of what in an imitative interaction? Frontiers in Human Neuroscience. 6:128 10.3389/fnhum.2012.00128

bioRxiv preprint doi: https://doi.org/10.1101/108878; this version posted February 15, 2017. The copyright holder for this preprint (which was not certified by peer review) is the author/funder. All rights reserved. No reuse allowed without permission.

Erla, S., Faes, L., Tranquillini, E., Orrico, D., & Nollo, G. (2009) Multivariate autoregressive model with instantaneous effects to improve brain connectivity estimation. Int J Bioelectromagn 11(2):74–79

Faes, L, & Nollo, G. (2010). Extended causal modelling to assess Partial Directed Coherence in multiple time series with significant instantaneous interactions. Biological Cybernetics, 103(5):387-400.

Faes, L., & Nollo, G. (2011). Multivariate frequency domain analysis of causal interactions in physiological time series. In Biomedical Engineering, Trends in Electronics, Communications and Software; AN Laskovski (ed); INTECH, pp. 403-428. ISBN: 978-953-307-475-7

Faes, L., Porta, A., & Nollo, G. (2010). Testing Frequency Domain Causality in Multivariate Time Series. IEEE Trans Biomed Eng, 57(8):1897-1906.

Farroni, T., Csibra, G., Simion, F., & Johnson, M. H. (2002). Eye contact detection in humans from birth. Proceedings of the National Academy of Sciences, U.S.A., 99, 9602–9605.

Feldman, R. (2006). From biological rhythms to social rhythms: Physiological precursors of mother-infant synchrony. Developmental psychology, 42(1), 175-188.

Feldman, R., Magori-Cohen, R., Galili, G., Singer, M., & Louzoun, Y. (2011). Mother and infant coordinate heart rhythms through episodes of interaction synchrony. Infant Behavior and Development, 34(4), 569-577.

bioRxiv preprint doi: https://doi.org/10.1101/108878; this version posted February 15, 2017. The copyright holder for this preprint (which was not certified by peer review) is the author/funder. All rights reserved. No reuse allowed without permission.

Franaszczuk, P.J., Blinowska, K.J., & Kowalczyk, M. (1985). The application of parametric multichannel spectral estimates in the study of electrical brain activity. Biol Cybern., 51:239–47.

Ganushchak, L.Y., & Schiller, N.O. (2008). Motivation and semantic context affect brain error-monitoring activity: an event-related brain potentials study. NeuroImage, 39, 395-405.

Giraud, A. L., & Poeppel, D. (2012). Cortical oscillations and speech processing: emerging computational principles and operations. Nat. Neurosci. 15, 511–51710.

Granger, C.W.J. (1969). Investigating causal relations by econometric models and cross-spectral methods. Econometrica, 37(3), 424-438.

Grossmann, T., Johnson, M.H., Farroni, T., & Csibra, G. (2007). Social perception in the infant brain: gamma oscillatory activity in response to eye gaze. Soc Cogn. Affect. Neurosci. 2, 284–291.

Hari, R., Himberg, T., Nummenmaa, L., Hämäläinen, M., & Parkkonen, L. (2013). Synchrony of brains and bodies during implicit interpersonal interaction. Trends in Cognitive Sciences, 17 (3), 105–106.

Hasson, U., Ghazanfar, A.A., Galantucci, B., Garrod, S. & Keysers, C. (2012). Brain-to-brain coupling as a mechanism for shared communication and cognition. Trends in Cognitive Sciences, 16: 114-121.

Hoehl, S., Michel, C., Reid, V. M., Parise, E., & Striano, T. (2014). Eye contact during live social interaction modulates infants' oscillatory brain activity. Social Neuroscience, 9(3), 300-308. doi: 10.1080/17470919.2014.884982

bioRxiv preprint doi: https://doi.org/10.1101/108878; this version posted February 15, 2017. The copyright holder for this preprint (which was not certified by peer review) is the author/funder. All rights reserved. No reuse allowed without permission.

Hoerzer, G.M., Liebe, S., Schloegl, A., Logothetis, N.K., & Rainer, G. (2010). Directed coupling in local field potentials of macaque v4 during visual short-term memory revealed by multivariate autoregressive models. Frontiers in Computational Neuroscience, 4:14. doi: 10.3389/fncom.2010.00014

Jansen B.H., Bourne J.R., & Ward J.W. (1981) Autoregressive estimation of short segment spectra for computerized EEG analysis. IEEE Trans. Biomedical Engineering. 28(9).

Jiang, J., Dai, B., Peng, D., Zhu, C., Liu, L., & Lu, C. (2012). Neural synchronisation during face-to-face communication. The Journal of Neuroscience, 32(45), 16064-16069.

Kampe, K. K., Frith, C. D., & Frith, U. (2003). "Hey John": signals conveying communicative intention toward the self activate brain regions associated with "mentalizing," regardless of modality. Journal of Neuroscience, 23(12), 5258-5263.

Kaye, K., & Fogel, A. (1980). The temporal structure of face-to-face communication between mothers and infants. Developmental Psychology, 16(5), 454.

Kayser, C., Ince, R.A., & Panzeri, S. (2012). Analysis of slow (theta) oscillations as a potential temporal reference frame for information coding in sensory cortices. PLoS Comput Biol. 8:e1002717.

Koike, T., Tanabe H.C., & Sadato, N. (2015). Hyperscanning neuroimaging technique to reveal the "two-in-one" system in social interactions. Neuroscience Research, 90, 25-32.

Koike, T., Tanabe, H.C., Okazaki, S., Nakagawa, E., Sasaki, A.T., Shimada, K., Sugawara, S.K., Takahashi, H.K., Yoshihara, K., Bosch-Bayard, J., & Sadato, N. (2016). Neural substrates of shared attention as social memory: a hyperscanning functional magnetic resonance imaging study, NeuroImage, 125, 401–412.

bioRxiv preprint doi: https://doi.org/10.1101/108878; this version posted February 15, 2017. The copyright holder for this preprint (which was not certified by peer review) is the author/funder. All rights reserved. No reuse allowed without permission.

Konvalinka I., Bauer M., Stahlhut C., Hansen L. K., Roepstorff A., & Frith C. D. (2014). Frontal alpha oscillations distinguish leaders from followers: multivariate decoding of mutually interacting brains. Neuroimage, 94, 79–88. 10.1016/j.neuroimage.2014.03.003

Kuhl,P.K. (2007). Is speech learning 'gated' by the social brain? Dev Sci.;10:110–120.

Kuhl, P., Tsao, F.-M., & Liu, H.-M. (2003). Foreign-language experience in infancy: Effects of short-term exposure and social interaction on phonetic learning. Proc Natl Acad Sci U S A., 100, 9096-9101.

Lachat F., Hugueville L., Lemaréchal J.-D., Conty L., & George N. (2012). Oscillatory brain correlates of live joint attention: a dual-EEG study. Front. Hum. Neurosci. 6:156. 10.3389/fnhum.2012.00156

Laganaro, M., & Perret, C. (2011). Comparing electrophysiological correlates of word production in immediate and delayed naming through the analysis of word age of acquisition effects. Brain Topogr., 24, 19-29.

Leong, V., Byrne, E., Clackson, K., Harte, N., Lam, S., de Barbaro, K., & Wass, S. (in revision). Infants' neural oscillatory processing of theta-rate speech patterns exceeds adults'.

Leslie, A. M. (1994). ToMM, ToBy, and agency: Core architecture and domain specificity in cognition and culture. In L. A. Hirschfeld & S. A. Gelman (Eds.), Mapping the mind: Domain specificity in cognition and culture. (pp.119-148). New York, NY: Cambridge University Press.

Lisman, J. (2005). The theta/gamma discrete phase code occuring during the hippocampal phase precession may be a more general brain coding scheme. Hippocampus. 15(7): 913-22.

bioRxiv preprint doi: https://doi.org/10.1101/108878; this version posted February 15, 2017. The copyright holder for this preprint (which was not certified by peer review) is the author/funder. All rights reserved. No reuse allowed without permission.

Luo, H., & Poeppel, D. (2007) Phase patterns of neuronal responses reliably discriminatespeech in human auditory cortex. Neuron, 54,1001–1010.

Marple, S.L., & Nuttall, A.H. (1983). Experimental comparison of three multichannel linear prediction spectral estimators, IEE Proc. F 130, 218–229

Meltzoff, A., & Moore, M. (1977). Imitation of Facial and Manual Gestures by Human Neonates. Science, 198(4312), 75-78.

Mundy, P., Card, J., & Fox, N. (2000). EEG correlates of the development of infant joint attention skills. Developmental Psychobiology. 36:325–338.

Mundy, P., Fox, N., & Card., J. (2003). Joint attention, EEG coherence and early vocabulary development. Developmental Science. 6:48–54.

Naeem M., Prasad G., Watson D. R., & Kelso J. A. S. (2012). Electrophysiological signatures of intentional social coordination in the 10-12 Hz range. Neuroimage 59 1795–1803. 10.1016/j.neuroimage.2011.08.010

Orekhova EV, Stroganova TA, Posikera IN. (1999). Theta synchronization during sustained anticipatory attention in infants over the second half of the first year of life. International Journal of Psychophysiology. 1999;32:151–172.

Parise, E., Friederici, A. D., & Striano, T. (2010). “Did you call me?” 5-month-old infants own name guides their attention. PLoS One, 5(12), e14208. doi:10.1371/journal.pone.0014208

Peelle, J.E., Gross, J., Davis, M.H. (2013) Phase-locked responses to speech in human auditory cortex are enhanced during comprehension. Cerebral Cortex 23:1378–1387.

bioRxiv preprint doi: https://doi.org/10.1101/108878; this version posted February 15, 2017. The copyright holder for this preprint (which was not certified by peer review) is the author/funder. All rights reserved. No reuse allowed without permission.

Porcaro, C., Medaglia, M.T., & Krott, A. (2015). Removing speech artifacts from electroencephalographic recordings during overt picture naming. NeuroImage, 105, 171-180.

Rogoff, B. (1990). Apprenticeship in thinking: Cognitive development in social context. New York, NY, US: Oxford University Press Apprenticeship in thinking: Cognitive development in social context. xiv 242 pp.

Saito, D.N., Tanabe, H.C., Izuma, K., Hayashi, M.J., Morito, Y., Komeda, H., Uchiyama, H., Kosaka, H., Okazawa, H., Fujibayashi, Y., Sadato, N. (2010). "Stay tuned": inter-individual neural synchronization during mutual gaze and joint attention. Front. Integr. Neurosci., p. 127 http://dx.doi.org/10.3389/fnint.2010.00127

Schack, B., Weiss, S., 2005. Quantification of phase synchronization phenomena and their importance for verbal memory processes. Biological Cybernetics 92, 275e287.

Schlogl, A. (2006). A comparison of multivariate autoregressive estimators. Signal Processing, 86:2426-2429.

Schroeder,C.E.,& Lakatos, P. (2009). Low-frequency neuronal oscillations as instruments of sensory selection. *Trends in Neurosciences*. 32, 9-18.

Senju, A., & Csibra, G. (2008). Gaze following in human infants depends on communicative signals. Current Biology, 18(9), 668-671.

Silbert, L.J., Honey, C.J., Simony, E., Poeppel, D., Hasson, U. (2014). Coupled neural systems underlie the production and comprehension of naturalistic narrative speech. Proceedings of the National Academy of Sciences, USA , 111(43):E4687-96.

bioRxiv preprint doi: https://doi.org/10.1101/108878; this version posted February 15, 2017. The copyright holder for this preprint (which was not certified by peer review) is the author/funder. All rights reserved. No reuse allowed without permission.

St. John, A.M., Kao, K., Choksi, M., Liederman, J., Grieve, P.G., & Tarullo, A.R. (2016). Variation in infant EEG power across social and nonsocial contexts. Journal of Experimental Child Psychology, 152, 106-122.

Stephens, G.J., Silbert, L.J., & Hasson, U. (2010). Speaker-listener neural coupling underlies successful communication. Proc Natl Acad Sci U S A.,107:14425–14430.

Striano, T., Reid, V., & Hoel, S. (2006). Neural mechanisms of joint attention in infancy. European Journal of Neuroscience. 23:2819–2823.

Schnitzler, A., Freund, H.-J., (1998). Detection of n:m phase locking from noisy data: application to magnetoencephalography. Physical Review Letters 81, 3291e3294.

Tanabe, H.C., Kosaka, H., Saito, D.N., Koike, T., Hayashi, M.J., Izuma, K., Komeda, H., Ishitobi, M., Omori, M., Munesue, T., Okazawa, H., Wada, Y., Sadato, N. (2012). Hard to "tune in": neural mechanisms of eye contact and joint attention in high-functioning autistic spectrum disorder. Front. Hum. Neurosci., 6, http://dx.doi.org/10.3389/fnhum.2012.00268

Telkemeyer S., Rossi S., Koch S. P., Nierhaus T., Steinbrink J., Poeppel D., Obrig H., Wartenburger I. (2009). Sensitivity of newborn auditory cortex to the temporal structure of sounds. J. Neurosci. 29, 14726–1473310.1523/JNEUROSCI.1246-09.2009

Vasios, C.E., Matsopoulos, G.K., Nikita, K.S., & Uzunoglu, N. (2003). Classification of event-related potentials using multivariate autoregressive modeling combined with simulated annealing. Journal of Automatic Control, University of Belgrade, 13(1), 7-11.

Vaz F., Guedes De Oliveira P., Principe J.C. (1987) A study on the best order for autoregressive EEG modelling. International Journal of Bio-Medical Computing. 20(1-2): 41-50.

bioRxiv preprint doi: https://doi.org/10.1101/108878; this version posted February 15, 2017. The copyright holder for this preprint (which was not certified by peer review) is the author/funder. All rights reserved. No reuse allowed without permission.

Werker, J.F. & Tees, R.C. (1984). Cross-language speech perception: evidence for perceptual reorganization during the first year of life. Inf Beh Dev,7, 49-63.

bioRxiv preprint doi: https://doi.org/10.1101/108878; this version posted February 15, 2017. The copyright holder for this preprint (which was not certified by peer review) is the author/funder. All rights reserved. No reuse allowed without permission.

SUPPLEMENTARY MATERIALS

Supplementary Methods

1 Nursery rhyme stimuli

	Duration (s) – Mean (std)		
	Direct gaze	Indirect gaze	Paired t-test p-value *(Bonferroni-corrected threshold = .007)*
Hickory Dickory Dock	7.34 (0.43)	7.31 (0.51)	.78
Humpty Dumpty	8.70 (0.61)	8.63 (0.63)	.23
Old MacDonald	19.63 (1.08)	19.49 (1.29)	.24
If You're Happy	13.84 (0.54)	13.88 (0.49)	.66
Wheels on the Bus	11.31 (0.53)	11.28 (0.40)	.66
Twinkle Little Star	21.62 (1.10)	21.39 (0.98)	.04
Where is Thumbkin	13.19 (0.73)	13.23 (0.62)	.65

Table S1. Duration of nursery rhyme stimuli used. Nursery rhymes were videoed live and the timings analysed post hoc. For each the average duration of each nursery rhyme during Direct and Indirect conditions is given. Paired sample t-tests were calculated to assess whether the average duration of any of the nursery rhymes was significant. No significant differences between conditions were identified.

bioRxiv preprint doi: https://doi.org/10.1101/108878; this version posted February 15, 2017. The copyright holder for this preprint (which was not certified by peer review) is the author/funder. All rights reserved. No reuse allowed without permission.

2 Description of EEG analyses methods

2.1 Computation of EEG power spectrum

As our main experimental goal was to assess changes in connectivity between gaze conditions, it was important to first establish whether there were any properties of the underlying EEG signal in each condition that might artifactually generate increases (or decreases) in computed connectivity. One such potential confounding factor is the composition of the power spectrum of the EEG signal. The accuracy of the partial directed coherence (PDC) metric can be sensitive to even moderate changes in signal-to-noise ratio (Adhikari et al, 2010). For example, Adhikari et al (2010) reported that a 10% decrease in signal power from 67% to 57% was associated with ~15% lower accuracy in PDC directionality estimation, although a similar 11% power change from 57% to 46% only caused an accuracy drop of <5%. Therefore, if the EEG signal in one experimental condition is more noisy than in another condition (or if the spectral composition of the signal changes substantially), this can lead to greater error in estimation of connectivity patterns. Accordingly, if we observed large changes in EEG power across conditions (e.g. a 10% drop in Alpha power), it would be important to bear in mind that any measured changes in PDC connectivity may be contaminated by estimation error.

To assess the power spectra of the EEG signals, their power spectral density (PSD) was estimated using the Matlab *'periodogram.m'* function, which performs a discrete Fourier transform on the signal. One PSD estimate was computed for each channel (left and right electrodes for adult and infant respectively), for each participant pair, and for each experimental condition. The resulting power spectra were then divided into EEG frequency bands, and averages were taken for each frequency band and used for analysis.

2.2 Neural connectivity analysis : Partial Directed Coherence (PDC)

Partial Directed Coherence (PDC) is a directional casual measure of direct flows between channels (Baccala & Sameshima, 2001; Baccala et al, 2007; Faes & Nollo, 2010, 2011). It based on the principles of Granger Causality (Granger, 1969), and measures the degree of influence that channel j (the 'Sender') *directly* has on channel i (the 'Receiver') with respect to the total influence of j on all channels in the network. Here, each individual electrode (Infant L, Infant R, Adult L, Adult R) was taken as one channel and the entire network consisted of 4 electrodes in total. We computed directed coherence values for all 12 possible pairwise connections, both within individual (e.g. Infant L -> Infant R) as well as across individuals (e.g. Infant L -> Adult L).

For the current analysis, we used Generalised Partial Directed Coherence (GPDC; Baccala et al, 2007), which is an adapted version of PDC with better variance stabilization properties and the advantage of scale-invariance (Hoerzer et al, 2010; Faes & Nollo, 2011). As a first step in the analysis, a multivariate autoregressive (MVAR) model is fitted to the EEG time series, which has the advantage of providing information about causal linear interaction effects in addition to estimating the coupling strength between channels. A frequency representation of the MVAR model parameters is then generated via a Fourier Transform, as follows:

$$A(f) = I - \sum_{p=1}^{P} A_p e^{-2\pi i p(\frac{f}{f_s})} \qquad \text{(eq.1)}$$

bioRxiv preprint doi: https://doi.org/10.1101/108878; this version posted February 15, 2017. The copyright holder for this preprint (which was not certified by peer review) is the author/funder. All rights reserved. No reuse allowed without permission.

where A_p are the model coefficients, I refers to the M-dimensional identity matrix, *fs* is the sampling frequency, and $i^2 = -1$. For each pair of channels (*i* and *j*), $GPDC_{ij}$ is then computed as :

$$GPDC_{ij}(f) = \frac{\frac{1}{\sigma_i}\,|A_{ij}(f)|}{\sqrt{\sum_{m=1}^{M} \frac{1}{\sigma_m{}^2}\,|A_{mj}(f)|^2}} \qquad \text{(eq.2)}$$

where σ_i^2 refers to the variance of the innovation process $x_i(t)$. GPDC takes values between [0,1] and is normalized across receivers (i.e. total outflow = 1 at each frequency), with larger values indicating strong connectivity.

The MVAR model was estimated using the Burg-type Nuttall-Strand method (Marple & Nuttall, 1983) which is thought to perform best for small sample sizes (Schlogl, 2006), and a model order (MO) of 5 was used. The model order (MO) indicates the number of preceding samples that are used to predict the data at sample time *t*, and determines the number of observed frequency components for each pair of channels, which is typically half the model order. Following prior studies on autoregressive modelling (Jansen et al, 1981; Vaz et al; 1987) and multivariate autoregressive modelling of EEG time series (Franaszczuk et al, 1985; Erla et al, 2009; Vasios et al, 2003; Anderson et al, 1998), here a model order of 5 was used for this analysis. For example, Jansen et al (1981) reported that a fifth order AR model was sufficient in 90% of cases to adequately capture variance in EEG time series data. Vaz et al (1987) also noted that *"a 5th order AR model represents adequately 1- or 2-s EEG segments with the exception of featureless background, where higher order models are necessary".* Model orders used in other MVAR EEG studies typically range between 3 and 6 (CW Anderson et al, 1998 [MO = 3]; Vasios et al, 2003 [MO = 4]; Erla et al, 2009 [MO = 5]; Franaszczuk et al, 1985 with 4 channels [MO = 6]).

One MVAR model and the resulting set of GPDC estimates (spanning the entire frequency spectrum) was computed for each non-overlapping 1.0s EEG epoch (200 data samples), and these estimate GPDC values were averaged across all epochs for each participant pair, for each experimental condition. The resulting epoch-averaged GPDC spectrum was then divided into five discrete EEG frequency bands using the banding commonly used in infant research (Delta [1-3 Hz], Theta [3-6 Hz], Alpha [6-9 Hz], Beta [9-25 Hz], and Gamma [25-40 Hz]) (Saby & Marshall, 2012). The mean GPDC value was taken within each frequency range, resulting in 5 summary GPDC indices for each pairwise connection, condition and participant. Note that as infants' Theta and Alpha EEG bands are lower in frequency as compared to adults (e.g. Orekhova et al, 1999), our frequency banding was adjusted lower accordingly.

Thresholds for significance testing were determined by generating a surrogate dataset comprising all possible combinations of *non-matched* adult-infant data. As there were four recording channels in total (Adult L and R, Infant L and R), the surrogate data were generated by selecting single channels from four separate, non-matching, participant pairs and cropping each to the shortest length of any single channel. For example, one possible combination was created by taking the Adult L channel from participant pair 1, the Adult R channel from participant pair 2, the Infant L channel from participant pair 3 and the Infant R channel from participant pair 4. As there were 19 matching participant pairs in the original dataset, this gave rise to 3876 possible combinations of non-matching data (19 choose 4). The identical directed coherence analysis was then performed on this surrogate dataset. The resulting mean

bioRxiv preprint doi: https://doi.org/10.1101/108878; this version posted February 15, 2017. The copyright holder for this preprint (which was not certified by peer review) is the author/funder. All rights reserved. No reuse allowed without permission.

values provided a baseline measure of the amount of 'random' coherence present between adult and infant EEG signals that did not specifically arise from the experimental task (e.g. due to all participants experiencing a similar physical testing environment). All GPDC analyses were performed using the eMVAR (Extended Multivariate Autoregressive Modelling) Toolbox (Faes & Nollo, 2011) in Matlab (The Mathworks Inc).

2.3 Computation of neural coherence to the speech stimulus

As the main analysis of brain-to-brain connectivity used partial directed coherence as the index, for comparability, a coherence index was also used to quantify neural encoding of speech temporal structure. Wavelet coherence (WCOH) quantifies the coherence between two time series as a function of both time and frequency (Torrence & Compo, 1998; Grinsted et al, 2004). This metric is well suited to investigating changes in coupling between nonstationary time series, and thus is particularly appropriate for use with neural data (Chang & Glover, 2010). WCOH utilises the continuous wavelet transform, which performs a time-frequency decomposition by convolving the time series with scaled and translated versions of a wavelet function (Mallat, 1999). Here, a complex Morlet wavelet was used (bandwidth of mother wavelet = 1 Hz, time resolution = 0.1 Hz) and the wavelet transform was computed at 7 frequencies, log-spaced between 0.5 Hz to 40 Hz. The Matlab function 'wcoher' (Mathworks, Inc) was used to estimate the wavelet coherence between the EEG signal and the speech amplitude envelope. WCOH values range between [0,1], and can be conceptualized as the localised correlation coefficient in time and frequency space (Grinsted et al., 2004).

bioRxiv preprint doi: https://doi.org/10.1101/108878; this version posted February 15, 2017. The copyright holder for this preprint (which was not certified by peer review) is the author/funder. All rights reserved. No reuse allowed without permission.

3 Summary of Mixed ANOVA design factors, predicted effects and interpretation

		Predicted Effect	**Interpretation**
Within-Subjects Factors	**Main Effects**		
	Gaze condition	Direct > Indirect	Overall network connectivity is stronger during Direct gaze
	Sender	Adult > Infant	Infants influence adults more strongly than the reverse
	Sending Hemi	No effect	No lateralization in sending
	Receiving Hemi	No effect	No lateralization in receiving
	Interaction Effects		
	Gaze x Sender	No interaction. i.e., *Ad Direct > Ad Avert* *Inf Direct > Inf Avert*	Both adults and infants influence each other more during Direct gaze
	Gaze x Sending Hemi	No interaction	Direct > Indirect for both sending hemispheres
	Gaze x Receiving Hemi	No interaction	Direct > Indirect for both receiving hemispheres
Between-Subjects Factors	**Main Effects**		
	Age Group	No effect	All infants show same pattern
	Interaction Effects		
	Age Group x Gaze condition	No interaction, i.e., *Young Direct > Young Avert* *Old Direct > Old Avert*	Direct > Indirect for infants of all ages
	Age Group x Sender	No interaction, i.e., *Adult > Young Infant* *Adult > Old Infant*	Both younger and older infants influence adults more

Table S2. Summary of Mixed ANOVA design factors, predicted effects and interpretation

bioRxiv preprint doi: https://doi.org/10.1101/108878; this version posted February 15, 2017. The copyright holder for this preprint (which was not certified by peer review) is the author/funder. All rights reserved. No reuse allowed without permission.

Supplementary Results

4 GPDC values by EEG frequency band

4.1 Across individuals

		Infant -> Adult				*Adult -> Infant*			
Sending Hemi		*L*		*R*		*L*		*R*	
Receiving Hemi		*L*	*R*	*L*	*R*	*L*	*R*	*L*	*R*
Delta (1-3 Hz)	Direct	**0.111**	**0.110**	**0.109**	**0.113**	**0.117**	**0.120**	**0.109**	**0.122**
		0.042	*0.028*	*0.028*	*0.036*	*0.032*	*0.032*	*0.020*	*0.029*
	Indirect	**0.115**	**0.110**	**0.106**	**0.111**	**0.110**	**0.120**	**0.116**	**0.109**
		0.029	*0.024*	*0.031*	*0.026*	*0.030*	*0.022*	*0.019*	*0.018*
Theta (3-6 Hz)	Direct	**0.072**	**0.070**	**0.071**	**0.072**	**0.068**	**0.067**	**0.060**	**0.068**
		0.025	*0.023*	*0.026*	*0.028*	*0.019*	*0.019*	*0.009*	*0.017*
	Indirect	**0.072**	**0.068**	**0.064**	**0.066**	**0.061**	**0.066**	**0.064**	**0.061**
		0.022	*0.019*	*0.017*	*0.019*	*0.017*	*0.015*	*0.012*	*0.011*
Alpha (6-9 Hz)	Direct	**0.075**	**0.072**	**0.077**	**0.080**	**0.042**	**0.041**	**0.037**	**0.041**
		0.022	*0.027*	*0.029*	*0.034*	*0.010*	*0.011*	*0.005*	*0.008*
	Indirect	**0.072**	**0.069**	**0.066**	**0.066**	**0.037**	**0.039**	**0.041**	**0.038**
		0.024	*0.025*	*0.027*	*0.023*	*0.010*	*0.007*	*0.010*	*0.008*
Beta (9-25 Hz)	Direct	**0.104**	**0.110**	**0.095**	**0.116**	**0.086**	**0.086**	**0.083**	**0.085**
		0.022	*0.050*	*0.019*	*0.048*	*0.013*	*0.015*	*0.018*	*0.010*
	Indirect	**0.095**	**0.095**	**0.090**	**0.093**	**0.083**	**0.086**	**0.086**	**0.080**
		0.020	*0.020*	*0.016*	*0.016*	*0.013*	*0.016*	*0.010*	*0.012*
Gamma (25-40 Hz)	Direct	**0.122**	**0.131**	**0.126**	**0.133**	**0.112**	**0.113**	**0.113**	**0.117**
		0.022	*0.052*	*0.028*	*0.034*	*0.016*	*0.011*	*0.015*	*0.018*
	Indirect	**0.121**	**0.124**	**0.114**	**0.122**	**0.113**	**0.111**	**0.114**	**0.113**
		0.015	*0.020*	*0.022*	*0.023*	*0.017*	*0.015*	*0.014*	*0.015*

*Table S3 – GPDC values by EEG frequency band across individuals (**mean** in bold, SD in italics)*

bioRxiv preprint doi: https://doi.org/10.1101/108878; this version posted February 15, 2017. The copyright holder for this preprint (which was not certified by peer review) is the author/funder. All rights reserved. No reuse allowed without permission.

4.2 Within individuals

		Infant -> Infant		*Adult -> Adult*	
Sending Hemi		*L*	*R*	*L*	*R*
Receiving Hemi		*R*	*L*	*R*	*L*
Delta (1-3 Hz)	Direct	**0.170**	**0.149**	**0.138**	**0.135**
		0.046	*0.033*	*0.035*	*0.033*
	Indirect	**0.159**	**0.157**	**0.139**	**0.128**
		0.038	*0.026*	*0.032*	*0.026*
Theta (3-6 Hz)	Direct	**0.110**	**0.100**	**0.077**	**0.075**
		0.038	*0.032*	*0.020*	*0.021*
	Indirect	**0.106**	**0.100**	**0.080**	**0.073**
		0.033	*0.025*	*0.022*	*0.018*
Alpha (6-9 Hz)	Direct	**0.104**	**0.101**	**0.048**	**0.049**
		0.038	*0.038*	*0.012*	*0.014*
	Indirect	**0.107**	**0.100**	**0.051**	**0.048**
		0.039	*0.035*	*0.014*	*0.014*
Beta (9-25 Hz)	Direct	**0.119**	**0.114**	**0.107**	**0.107**
		0.031	*0.040*	*0.012*	*0.016*
	Indirect	**0.121**	**0.123**	**0.110**	**0.111**
		0.028	*0.047*	*0.023*	*0.022*
Gamma (25-40 Hz)	Direct	**0.135**	**0.132**	**0.119**	**0.117**
		0.029	*0.028*	*0.017*	*0.017*
	Indirect	**0.138**	**0.135**	**0.114**	**0.114**
		0.031	*0.030*	*0.020*	*0.016*

*Table S4 – GPDC values by EEG frequency band within individuals (**mean** in bold, SD in italics)*

bioRxiv preprint doi: https://doi.org/10.1101/108878; this version posted February 15, 2017. The copyright holder for this preprint (which was not certified by peer review) is the author/funder. All rights reserved. No reuse allowed without permission.

5 Full ANOVA Results

5.1 Across individuals

		Delta F(1,16) =	**Theta** F(1,16) =	**Alpha** F(1,16) =	**Beta** F(1,16) =	**Gamma** F(1,16) =
Within-Subjects Factors	**Main Effects**					
	Gaze condition	2.29, p = .15 η^2p = *.13*	***5.40, p<.05** η^2p = *.25*	***7.94, p<.05** η^2p = *.33*	***7.95, p<.05** η^2p = *.33*	2.39, p = .14 η^2p = *.13*
	Sender	0.02, p = .90 η^2p = *.00*	0.56, p = .46 η^2p = *.03*	***7.35, p<.05** η^2p = *.32*	***7.41, p<.05** η^2p = *.32*	2.87, p = .11 η^2p = *.15*
	Sending Hemi	0.72, p = .41 η^2p = *.04*	0.75, p = .40 η^2p = *.04*	1.02, p = .33 η^2p = *.06*	0.04, p = .84 η^2p = *.00*	0.60, p = .45 η^2p = *.04*
	Receiving Hemi	1.22, p = .29 η^2p = *.07*	0.27, p = .61 η^2p = *.02*	0.87, p = .37 η^2p = *.05*	0.14, p = .71 η^2p = *.00*	1.81, p = .20 η^2p = *.10*
	Interaction Effects					
	Gaze x Sender	0.16, p = .70 η^2p = *.01*	0.13, p = .73 η^2p = *.01*	4.01, p = .06 η^2p = *.20*	4.30, p = .05 η^2p = *.21*	2.14, p = .16 η^2p = *.12*
	Gaze x Send Hemi	0.37, p = .55 η^2p = *.02*	1.73, p = .21 η^2p = *.10*	0.82, p = .38 η^2p = *.05*	2.06, p = .17 η^2p = *.11*	0.12, p = .73 η^2p = *.01*
	Gaze x Rec Hemi	0.00, p = .95 η^2p = *.00*	0.02, p = .89 η^2p = *.00*	0.11, p = .75 η^2p = *.01*	0.39, p = .54 η^2p = *.02*	1.82, p = .20 η^2p = *.10*
Between-Subjects Factors	**Main Effects**					
	Age Group	0.16, p = .70 η^2p = *.01*	0.17, p = .69 η^2p = *.01*	0.03, p = .87 η^2p = *.00*	0.69, p = .42 η^2p = *.04*	0.48, p = .50 η^2p = *.03*
	Interaction Effects					
	Age Group x Gaze	0.22, p = .65 η^2p = *.01*	0.53, p = .48 η^2p = *.03*	1.02, p = .33 η^2p = *.06*	1.55, p = .23 η^2p = *.09*	1.03, p = .33 η^2p = *.06*
	Age Group x Sender	0.76, p = .40 η^2p = *.05*	0.34, p = .57 η^2p = *.02*	0.13, p = .73 η^2p = *.01*	0.20, p = .66 η^2p = *.01*	1.45, p = .25 η^2p = *.08*

*Table S5 – Full ANOVA results from Mixed Design ANOVAs examining across-individual effects, conducted as described in the main text. * p<.05*

bioRxiv preprint doi: https://doi.org/10.1101/108878; this version posted February 15, 2017. The copyright holder for this preprint (which was not certified by peer review) is the author/funder. All rights reserved. No reuse allowed without permission.

5.2 Within individuals

		Delta	**Theta**	**Alpha**	**Beta**	**Gamma**
Within-Subjects Factors	**Main Effects**					
	Gaze condition	***4.83, p<.05** η^2p = *.23*	4.31, p = .05 η^2p = *.21*	0.03, p = .87 η^2p = *.00*	0.38, p = .55 η^2p = *.02*	1.34, p = .26 η^2p = *.08*
	Sender	***6.18, p<.05** η^2p = *.28*	****8.80, p<.01** η^2p = *.35*	****12.0, p<.01** η^2p = *.43*	3.13, p = .10 η^2p = *.16*	***6.33, p<.05** η^2p = *.28*
	Hemi direction	1.63, p = .22 η^2p = *.09*	1.27, p = .28 η^2p = *.07*	1.79, p = .20 η^2p = *.10*	0.01, p = .93 η^2p = *.00*	0.57, p = .46 η^2p = *.03*
	Interaction Effects					
	Gaze x Sender	0.02, p = .88 η^2p = *.00*	0.14, p = .72 η^2p = *.01*	1.68, p = .21 η^2p = *.10*	0.48, p = .50 η^2p = *.03*	1.22, p = .29 η^2p = *.07*
	Gaze x Hemi	1.19, p = .29 η^2p = *.07*	0.21, p = .66 η^2p = *.01*	0.95, p = .34 η^2p = *.06*	0.33, p = .58 η^2p = *.02*	0.20, p = .66 η^2p = *.01*
Between-Subjects Factors	**Main Effects**					
	Age Group	0.88, p = .36 η^2p = *.05*	0.29, p = .60 η^2p = *.02*	0.07, p = .80 η^2p = *.00*	0.81, p = .38 η^2p = *.05*	0.21, p = .65 η^2p = *.01*
	Interaction Effects					
	Age Group x Gaze	0.01, p = .93 η^2p = *.00*	1.27, p = .28 η^2p = *.07*	1.76, p = .20 η^2p = *.10*	0.07, p = .79 η^2p = *.00*	0.24, p = .63 η^2p = *.01*

*Table S6 – Full ANOVA results from Mixed Design ANOVAs examining within-individual effects, conducted as described in the main text. * p<.05, **p<.01. Note that for these within-individual analyses, the factor of 'Sender' referred to whether intra-personal connectivity was being computed for the Infant or Adult brain.*

bioRxiv preprint doi: https://doi.org/10.1101/108878; this version posted February 15, 2017. The copyright holder for this preprint (which was not certified by peer review) is the author/funder. All rights reserved. No reuse allowed without permission.

5.3 Summary of within-individual connectivity effects

The main Results section (3.3) describes the results of the analyses examining across-individual connectivity. Here we present the results of identical tests examining within-individual connectivity (i.e. infant L -> infant R, adult L -> adult R).

Stronger Delta within-brain connectivity for Direct gaze. When assessing within-individual connectivity patterns as a function of gaze, our results revealed that in the Delta band, overall within-brain neural connectivity was higher for Direct than Indirect gaze ($F(1,16) = 4.83$, $p<.05$, $\eta^2p = .23$). However, this pattern was not observed at any other frequency (Table S6). Further there was no significant interaction between gaze and any other factor in the Delta band (or at any other frequency), suggesting that the pattern of increased within-brain Delta connectivity was consistent across adults and infants, hemispheres and infant age groups.

Stronger within-brain connectivity in infants than adults. When comparing the within-brain connectivity strength of infants and adults (i.e. Sender effect for within-individual analyses), we observed that in four out of the five frequency bands assessed (except for Beta), infants showed stronger within-brain (L-R) connectivity than adults (Delta : $F(1,16) = 6.18$, $p<.05$, $\eta^2p = .28$; Theta : $F(1,16) = 8.80$, $p<.01$, $\eta^2p = .35$; Alpha : $F(1,16) = 12.0$, $p<.01$, $\eta^2p =.43$; Beta : $F(1,16) = 3.13$, $p=.10$, $\eta^2p = .16$; Gamma : $F(1,16) = 6.33$, $p<.05$, $\eta^2p = .28$).

5.4 Summary of age effects

No effect of infant age. We also examined the effect of age based on a median split analysis that divided our data into younger and older infants. Across all analyses conducted, both between- and within-individuals, there were no significant differences observed between younger and older infants, and no interaction between age and any other factor (see Tables S5 and S6). Thus, the reported effects of gaze, direction of influence and connectivity strength did not differ as a function of infants' age.

bioRxiv preprint doi: https://doi.org/10.1101/108878; this version posted February 15, 2017. The copyright holder for this preprint (which was not certified by peer review) is the author/funder. All rights reserved. No reuse allowed without permission.

6 Neural coherence to speech

Finally, in order to assess whether any *interpersonal* connectivity gaze effects could be attributed to differences in basic speech processing across gaze conditions, we examined whether neural oscillatory coherence to the amplitude envelope (temporal structure) of the adult's speech signal differed between gaze conditions. Figure S1 shows the strength of coherence for infants (red) and adults (blue), for Direct gaze (solid line) and Indirect gaze (dashed line), for left and right hemispheres (left and right subplots), at each of 7 frequencies from 0.5-40 Hz.

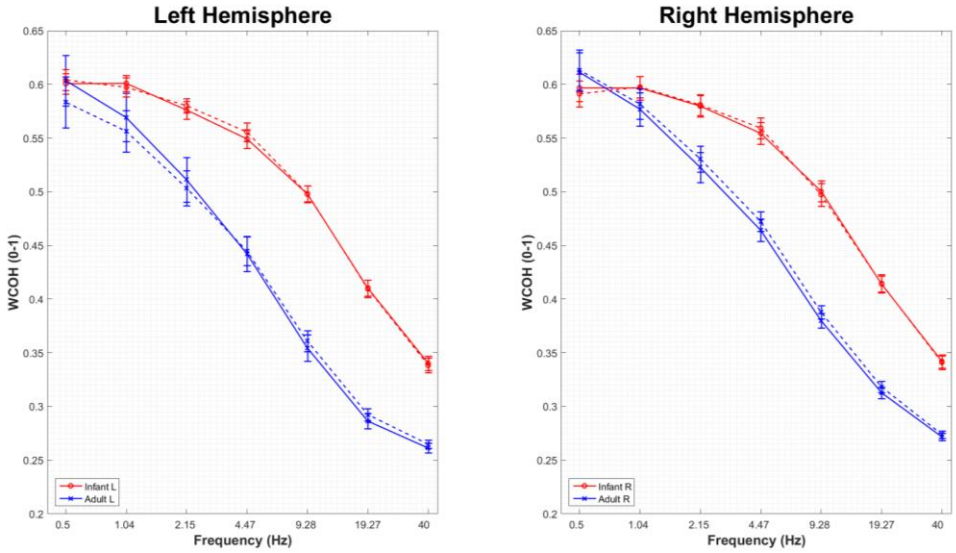

Figure S1. Speech-brain coherence values for adults and infants by condition and hemisphere (left hemisphere = left subplot, right hemisphere = right subplot). Frequency is shown on the x-axis and coherence value is shown on the y-axis. Adults are plotted in blue and infants are plotted in red. Solid lines indicate Direct gaze and dashed lines indicate Indirect gaze. Error bars show the standard error of the mean.

An ANOVA was conducted taking Gaze (Direct or Indirect), Hemisphere (Left or Right) and Frequency (7 Frequencies) as within-subjects factors, and Group (Infant or Adult) as the between-subjects factor. There was *no* significant difference in speech-brain coherence between Direct and Indirect gaze conditions ($F(1, 36)=.09$, $p=.76$). Further, there was no significant interaction between Gaze and any other factor (Gaze x Group : $F(1, 36)=.02$, $p=.88$; Gaze x Hemisphere : $F(1, 36)=.81$, $p=.37$; Gaze x Frequency : $F(6, 216)=1.50$, $p=.18$), suggesting that gaze did not change the pattern of speech-brain coherence for infants or adults in either hemisphere, at any frequency. Therefore, any *interpersonal* connectivity gaze effects cannot be attributed to differences in basic speech processing by either infants or adults. Consistent with our previous findings (Leong et al, under revision), we also observed, as an independent finding, that infants' overall strength of neural coherence to speech was significantly higher than adults' ($F(1, 36)=34.11$, $p<.001$).

bioRxiv preprint doi: https://doi.org/10.1101/108878; this version posted February 15, 2017. The copyright holder for this preprint (which was not certified by peer review) is the author/funder. All rights reserved. No reuse allowed without permission.

Supplementary Discussion

7 Discussion of EEG artifacts

Speech production artifacts were present in the EEG signal of the adult speaker, and these articulatory motions are known to reduce the signal-to-noise ratio of neural signals that relate to cognition (Brooker & Donald, 1980). For instance, the temporalis muscle is used for closing the lower jaw and this muscle spreads widely over the scalp locations that correspond to the frontal/temporal/parietal junction of the brain, generating large artifacts in the EEG signals measured over these regions (Brooker and Donald, 1980). Muscle artifact contamination is greatest over frontal and temporal scalp regions (De Vos et al, 2010) and generally less severe over central regions, where our recording electrodes were placed. Several methods have been proposed for removing speech artifacts from the EEG signal. These include the use of low-pass filtering to remove muscle artifacts that most prominently occur at frequencies over 12 or 20 Hz (Ganushchak and Schiller, 2008; Laganaro and Perret, 2011), and blind source separation based on Canonical Correlation Analysis (De Vos et al, 2010) or Independent Component Analysis (Porcaro et al, 2015) to separate cortical sources from electromyographic (EMG) responses. However, none of these methods are able to completely remove motion artifacts from the EEG signal, and may even remove some genuine neural activity of interest. In the current analysis, no specific methods were used to remove motion artifacts from the adult EEG (although standard artifact rejection for amplitudes >+100 μV was applied). Therefore, some articulatory artifacts will have been present in the adult EEG signal.

However, in the current study, the crucial comparison was the *difference* between Direct and Indirect gaze conditions, and not the neural activity per se in any one condition. As the adult speaker was uttering the same nursery rhymes in both Direct and Indirect gaze conditions, the quantity and magnitude of her articulatory artifacts would be matched across conditions and should not bias our results towards any one condition. Also, motion artifacts were only present in the adult's EEG data, and not in infants' EEG data, as segments with infant motion were excluded from analysis. Since only one partner in the dyad was moving while the other was still, this excludes the possibility of motion-related motor synchronization between partners (e.g. when both partners are speaking or moving at the same time). If motion synchronization had occurred, observed levels of neural synchrony could have been artifactually increased because these motion artifacts would be present with a similar temporal pattern in both partners' EEG time series. Therefore, although motion artifacts were present in the adult's EEG signal, we do not expect this to have artifactually increased levels of observed interpersonal neural coupling, or to have biased our findings toward a particular gaze condition.